JOURNAL of
MATERIALS and MECHATRONICS:A

e-ISSN 2717-8811
JournalMM, 2022, 3(1), 129-136
https://doi.org/10.55546/jmm.1072466

Araştırma Makalesi / Research Article

Reactive Sintering of Boron Carbide Based Ceramics by SPS

Hülya BİÇER [1]*

[1] Kütahya Dumlupınar Üniversitesi, Mühendislik Fakültesi, Metalurji ve Malzeme Mühendisliği Bölümü, Kütahya Türkiye,
ORCID ID: https://orcid.org/0000-0001-6633-7085, hulya.bicer@dpu.edu.tr

Geliş/ Received: 12.02.2022; **Kabul / Accepted:** 22.05.2022

ABSTRACT: Boron carbide is a highly covalent non-oxide ceramic with a high melting temperature. Therefore, the densification of boron carbide via a thermally activated process is extremely hard and requires additional driving forces. In addition to searching alternative production techniques for boron carbide, the production of boron carbide composites is one of the most interested subjects. In this study, B_xC-TiB_2-SiC ceramic was produced through an in-situ reaction between B_4C and Ti_3SiC_2 and excess amorphous boron using spark plasma sintering method at 1600°C-1800°C. XRD and microstructure analysis of the sintered sample show that boron rich boron carbide phase is present in the sintered specimen, which did not develop a continuous matrix through the sample. The three phases present in ceramics formed agglomerate throughout the microstructure and did not show homogeneous distribution.

Keywords: Boron carbide, Composite, Reactive sintering.

*Sorumlu yazar / Corresponding author: hulya.bicer@dpu.edu.tr

Bu makaleye atıf yapmak için /To cite this article

Biçer, H. (2022). Reactive Sintering of Boron Carbide Based Ceramics by SPS. Journal of Materials and Mechatronics: A (JournalMM), 3(1), 129-136.

1. INTRODUCTION

Boron carbide (B_4C) is an important non-oxide ceramic with high hardness, excellent thermal and electrical properties, and high chemical inertness. B_4C is used as ceramic armor due to its high strength to weight ratio and used as abrasion coating due to its high abrasion resistance. On the other hand, low fracture toughness impedes the application of B_4C in a broad range of areas (Thevenot, et al., 1990; Domnich et al., 2011; Biçer et al.,2020). Moreover, due to the covalent nature of its bonds, the sintering of B_4C is extremely difficult and requires high sintering temperature and long time. To overcome these limitations, alternative advanced sintering techniques are adopted. Spark plasma sintering is an electric field-assisted method that promises densification at lower temperatures and shorter times for high melting ceramics. One of the main advantages of spark plasma sintering of B_4C is reducing grain growth (Angers and Beauvy, 1984; Munir et al., 2006). The introduction of second phases into the B_4C matrix is another alternative to reduce the sintering temperature and improve the mechanical properties of B_4C. These phases, such as TiB_2, ZrB_2, SiC, ZrO_2, Al_2O_3, etc., effectively enhance the strength of B_4C by producing composite with toughening phase. In particular, TiB_2 and SiC are of interest to researchers. Both phases improve the toughness of B_4C while preserving its high hardness (Skorokhod et al., 1996; Ye et al., 2010; Zhang et al., 2017; Yin et al, 2018; Ding et al., 2019). The direct addition of TiB_2 and SiC phases into B_4C is likely to contribute to the aggregation explained in reference (Liu et al, 2020). Researchers have produced B_4C based composite with TiB_2 and SiC by reactive sintering techniques. SPS is an excellent method to produce a composite with *in-situ* reactive sintering. The metallic phase in the sintering aid promotes liquid phase sintering during the densification route. B_4C-TiB_2-SiC composite was produced by Wen et al. by hot-press using Ti_3SiC_2 as an additive and increased the fracture toughness to 8MPa $m^{1/2}$ (Wen et al, 2017). Song et al. fabricated B_4C-TiB_2-SiC composite with the addition of 5% (Ti_3SiC_2+Si) by spark plasma sintering and obtained 38.4 GPa hardness and 5.61 MPa $m^{1/2}$ fracture toughness (Song et al, 2020). In this study, B_xC-TiB_2-SiC composites were fabricated by reactive spark plasma sintering with Ti_3SiC_2 MAX phase. At higher temperatures Ti_3SiC_2 decomposes and reacts with B_4C to produce TiB_2 and SiC phases and additional carbon. To maintain B_4C in the structure, B content is also increased by adding excess B.

2. MATERIALS AND METHODS

Boron carbide (< 5 μm, %98.5 purity, H. C. Starck), Ti_3SiC_2 (< 10 μm, %99 purity, Kanthal), and amorphous boron (≤1 μm, ≥95%, Sigma Aldrich) are starting powders. The molar ratio of B_4C to Ti_3SiC_2 powder is 1:2, and excess amorphous boron was also added in ethanol for 5 hours by ball milling. Silicon carbide balls were used with a ball/powder weight ratio of 0.25. The mixture was dried at 80°C for 36 hours, and then the obtained powders were sieved. The SEM images of starting powders (B_4C and Ti_3SiC_2) are shown in figure 1. The particle size analysis of powder mixture was carried out by IMAGEJ software (NIH) from the SEM images taken at different magnifications. Powders were weighed and inserted into a 20 mm diameter graphite mold and densified by the FCT HP D 25-SD spark plasma sintering furnace. The SPS process was carried out in a vacuum under uniaxial pressure at different temperatures. An initial pressure of 5.6kN (15MPa) was applied up to 500°C and then the pressure was increased gradually to 22kN (50MPa) and maintained. The heating rate was rapid up to 1500°C (200°C/min). The sample was held for 2 min at 1500°C while the heating rate was decreased to 50°C/min. Prepared powder mixture was sintered at 1600 °C, 1700 °C, and 1800 °C with 10 min. dwelling time. The phase analysis was performed with XRD (PANALYTICAL-

EMPYREAN), and the microstructures were examined with the scanning electron microscope (NOVA).

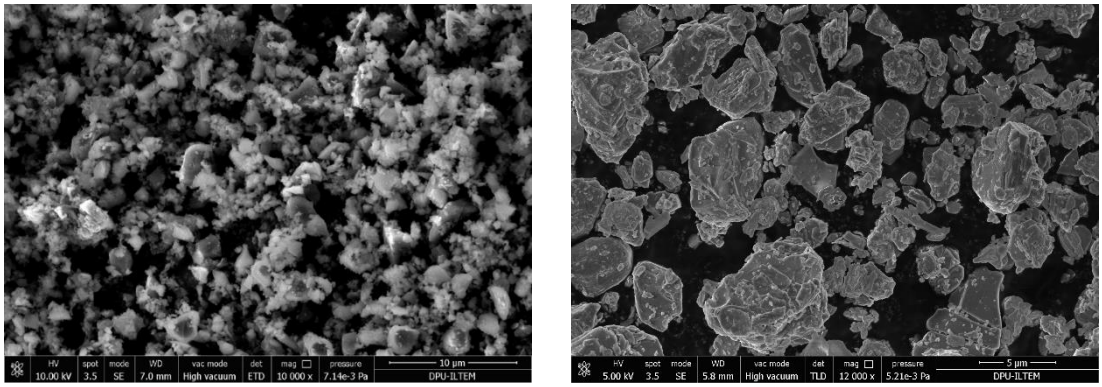

Figure 1. Microstructure of starting powder (left: boron carbide, right: MAX phase)

3. RESULTS AND DISCUSSION

XRD pattern and SEM image of the mixed powder are given in figure 2. The particle size of mixed powder after milling is less than 3 μ (Çanakçı et al, 2013). No sign of any contamination in the powder mixture after milling was detected by XRD analysis. Large particles of MAX phase were grinded into smaller particles while keeping the initial morpholgy. The theoretical density of the samples, corresponding to the full density products without pores, calculated from the weight fraction and density of each component is approximately 3.3 g/cm^3. The density of the sintered samples was calculated by using the Archimedes method. The samples were boiled and the volume of the sample was taken as the mass difference between the wet weight and the suspended weight. The sample sintered at 1600 ℃, 1700 ℃ and 1800℃ resulted in 3.20g/cm^3, 3,24 g/cm^3, and 3,25g/cm^3 respectively.

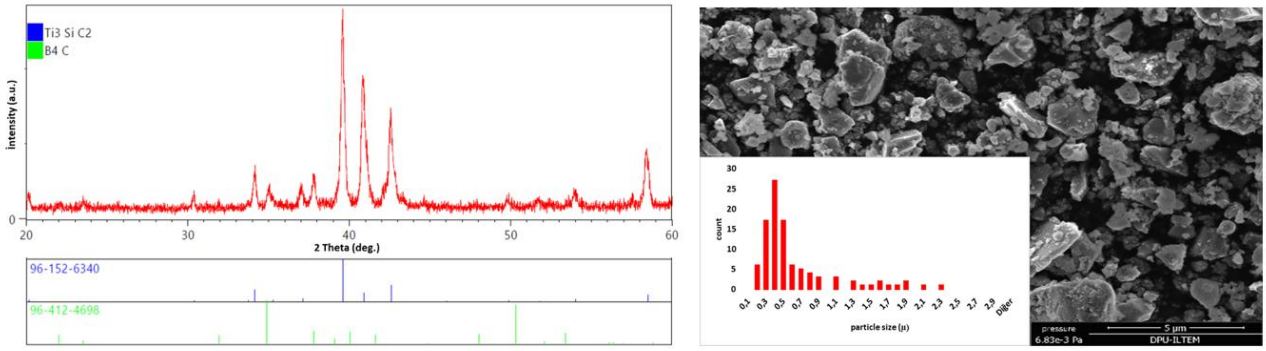

Figure 2. XRD pattern and SEM image of mixed powder after milling

The effect of temperature on the phase composition is presented in figure 3. The peaks in the XRD patterns belong to B_xC, TiB_2, SiC, TiC_x, and C phases. In the sample sintered at 1600°C, the peak of the TiC_x phase, which was formed as a result of the decomposition of Ti_3SiC_2, was observed. At higher temperatures, the TiC_x phase fully dissappears trough the reaction with B_4C to produce TiB_2. When the temperature was increased from 1600°C to 1800°C, TiB_2 peak became more distinctive. Free carbon exists in the boron carbide starting powder and graphite die used in SPS possibly contribute to the formation of SiC and boron carbide phases. The comparison of (104)

reflection of boron carbide for pure boron carbide and mixed powder, both sintered at 1700 °C is shown in figure 4 which shows the peak shift in (104) reflection towards lower angles for boron carbide, which is due to the distortion of boron carbide lattice by the boron substitution of carbon (Aselage and Tissot, 1992). Following reaction is predicted for the formation of TiB_2 and SiC phases, and the addition of excess boron promotes the existence of boron carbide in the structure (He et al.,2019).

$$3B_4C + 2Ti_3SiC_2 \rightarrow 6TiB_2 + 2SiC + 5C \quad (1)$$

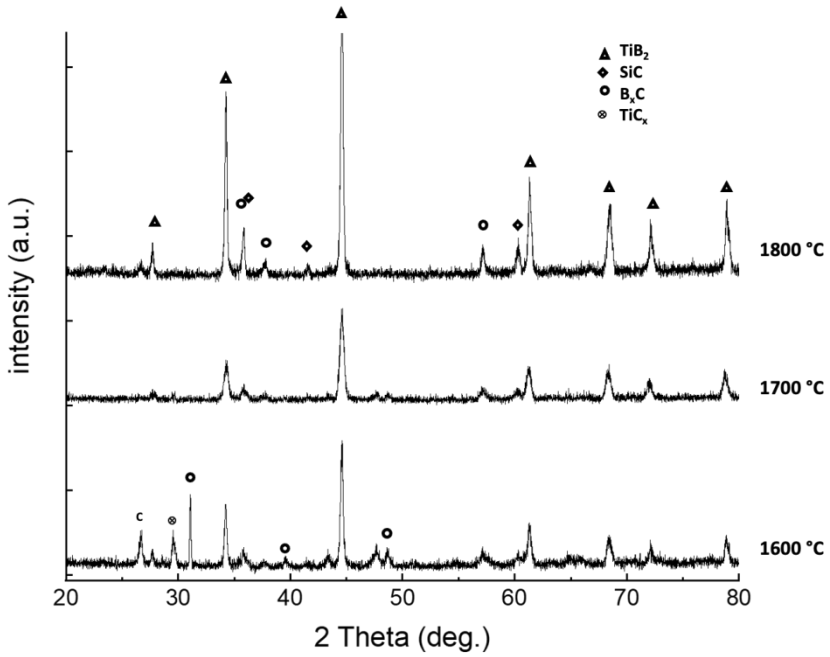

Figure 3. XRD patterns of the samples sintered at 1600°C, 1700°C, and 1800°C

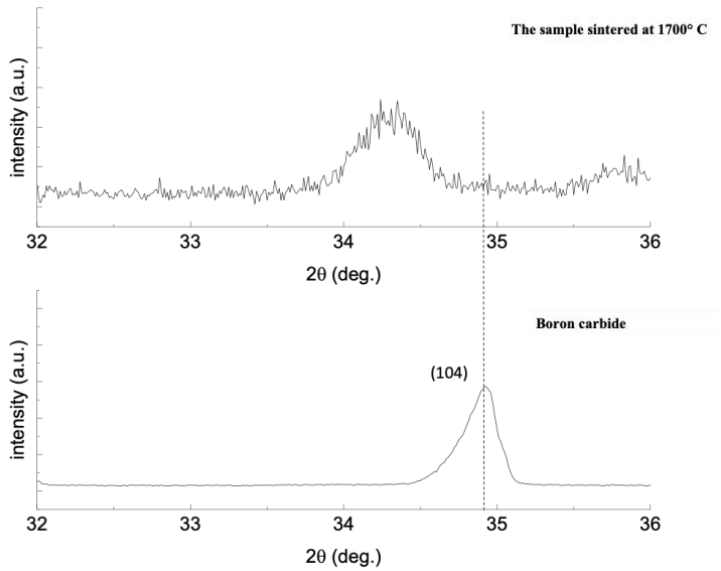

Figure 4. (104) reflection of boron carbide phase in the sample sintered at 1700°C is shown comparing boron carbide which was also sintered at 1700°C

SPS piston displacement, mechanical load, and sample temperature as a function of time during the consolidation of powders is presented in figure 5. In the SPS, the shrinkage can be estimated from

the displacement of the upper piston of the pressing tools (positive displacement). Initially, the pre-mixed powder was compacted with 5.6kN (15MPa) pressure up to 500°C. The pressure was increased gradually to 22kN (50MPa) afterward. The conjugated effect of temperature and pressure leads to the densification of the sample beginning from 1500 °C. The densification rate decreased while temperature and pressure were constant at dwelling temperature (1600-1800°C). Higher shrinkage in the sample at higher temperatures was observed, compromising density measurement.

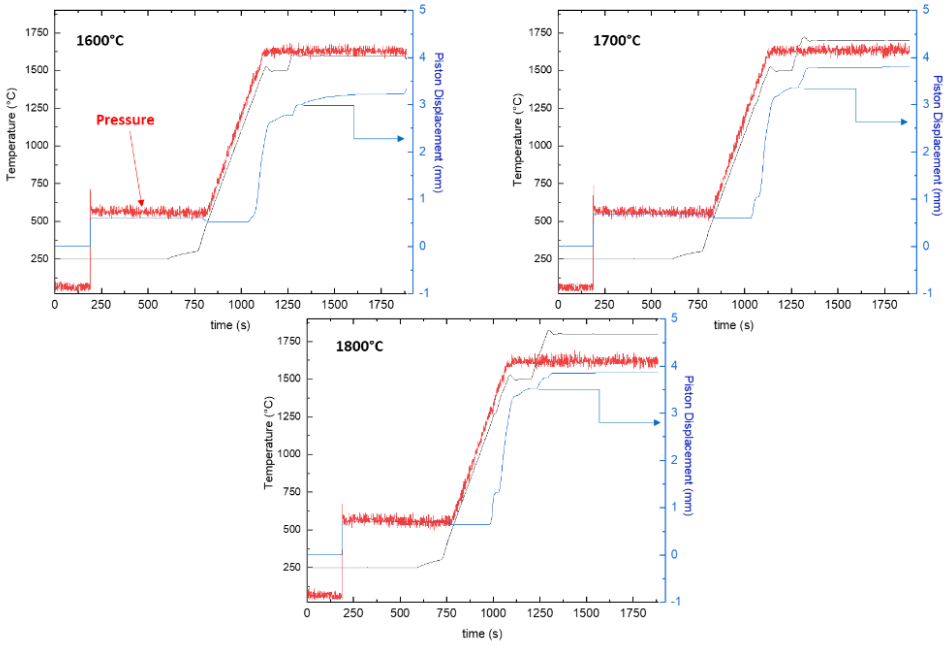

Figure 5. The sintering conditions (piston displacement, load, and temperature) as a function of time during SPS

Microstructure analysis on the fractured surface of the specimen and BSE image of the sample sintered at 1800 °C is shown in figure 6. The sample sintered at 1600 °C has the lowest density. Clusters of particles and weak particle-matrix bonding can be observed from microstructures (figure 6 e and f). The samples sintered at 1700°C and 1800°C show lower amount of porosity. The appearance of the dimples on the fracture surface indicates a ductile fracture mechanism. The microstructure of the sintered sample demonstrates that the light grey phase is TiB_2 (high atomic number), grey areas are SiC phase, and dark phases are presumably boron carbide. Figure 7 shows the elemental mapping of the fracture surface of sample sintered at 1800°C. Titanium and silicon deficiencies can be observed in regions rich in carbon and boron. In regions enriched with Ti and B, C and Si appears to be absent. In general, agglomerates are more apparent and non-homogeneously distributed throughout the microstructure. BSE images (sensitivity to differences in atomic number) of the sample sintered at 1800°C in figure 6 (e and f) also support the result. He et al. observed homogenously dispersed continuous boron carbide matrix by adding different amount of Ti_3SiC_2 into boron carbide (He et al, 2016). In this study, boron carbide does not form a continuous matrix in the microstructure.

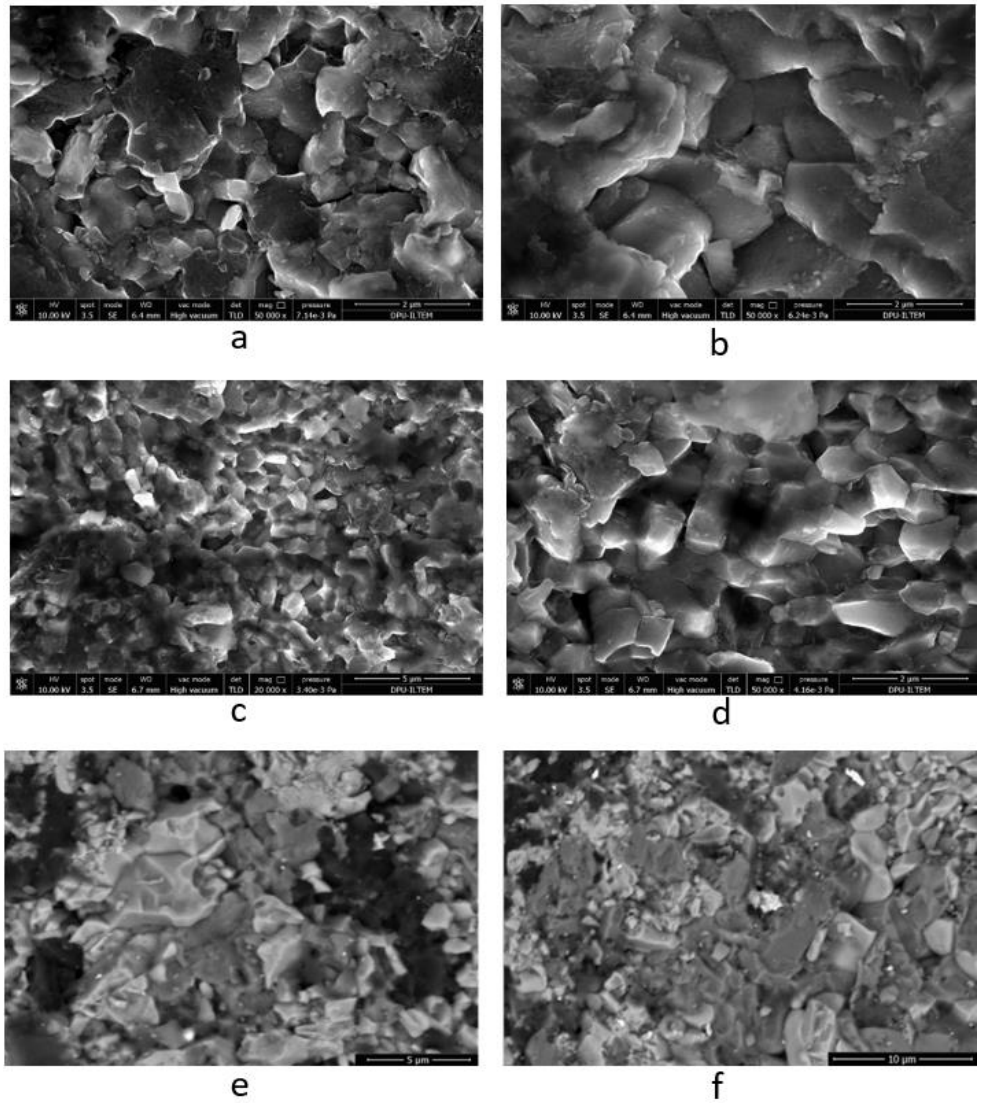

Figure 6. Microstructure of the samples sintered at (a) 1600°C, (b) 1700°C, (c) and (d) 1800°C. (e) and (f) are BSE images of the sample sintered at 1800°C

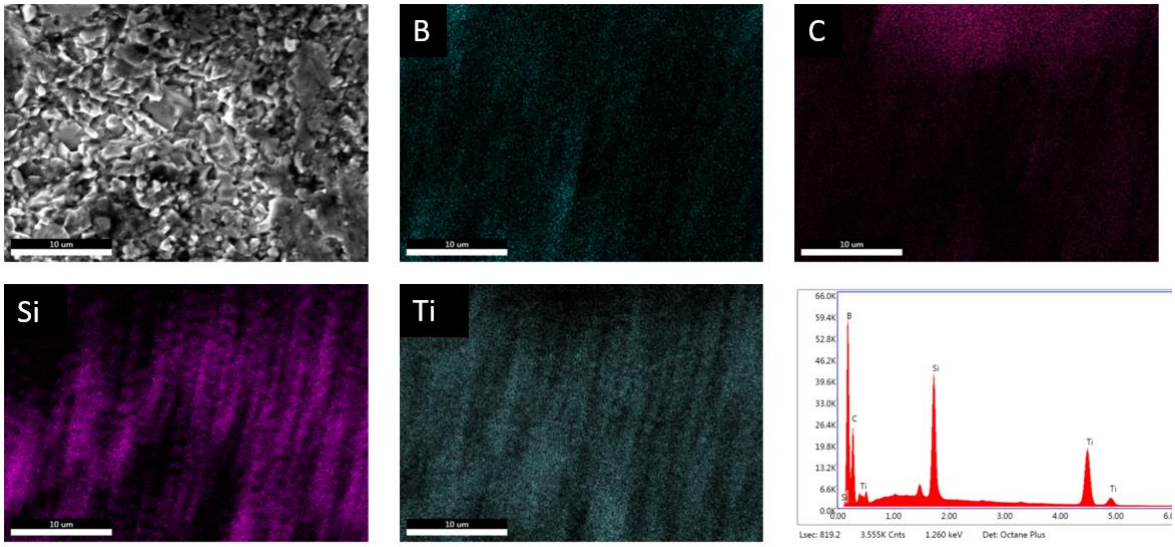

Figure 7. The SEM image of the fractured surface of the sample sintered at 1800°C, along with the attributing EDX maps.

4. CONCLUSIONS

This study reports spark plasma sintering behavior of boron carbide using Ti_3SiC_2 and excess amorphous boron as sintering additives. The addition of Ti_3SiC_2 in B_4C induced the formation of TiB_2, and SiC phases by reactive sintering. Higher sintering temperature yields to higher densification which can be observed from SPS data and the microstructure of the samples. BSE images and elemental mapping show that the all three phases are not uniformly distributed throughout the microstructure. The presence of the dimples on the fractured surface of the samples indicates the ductile structure of the produced samples. It is known that the increase of the volume fraction of B_xC in the ceramic by addition of excess boron leads the higher hardness. In order to investigate the effect of B excess on the mechanical properties of the composite, further studies will be carried out with different B/MAX phase ratios.

5. ACKNOWLEDGEMENTS

This study was supported by Kütahya Dumlupinar University Scientific Research Projects Commission, project 2017-67 and YOK-MEVLANA PROJECT (MEV.2018-9999). Author also would like to thank Prof. Dr. Hasan Göçmez and Prof. Dr. Mustafa Tuncer for their valuable contrubitions.

6. CONFLICT OF INTEREST

Author approves that to the best of their knowledge, there is not any conflict of interest or common interest with an institution/organization or a person that may affect the review process of the paper.

7. AUTHOR CONTRIBUTION

Hülya BİÇER has the full responsibility of the paper about determining the concept of the research, data collection, data analysis and interpretation of the results, preparation of the manuscript and critical analysis of the intellectual content with the final approval.

8. KREFERENCES

Angers R., Beauvy M., Hot-pressing of boron carbide, Ceramics international 10(2), 49-55, 1984.

Aselage T. L, Tissot R. G., Lattice constants of boron carbides. Journal of the American Ceramic Society 75 (8), 2207-2212, 1992.

Biçer H., Akdoğan E., Şavklıyıldız İ, Haines C., Zhong Z., Tsakalakos T., Thermal expansion of nano–boron carbide under constant DC electric field: An in situ energy dispersive X-ray diffraction study using a synchrotron probe. Journal of Materials Research 35(1), 90-97, 2020.

Canakci A., Erdemir F., Varol T., Patir A., Determining the effect of process parameters on particle size in mechanical milling using the Taguchi method: measurement and analysis. Measurement 46(9), 3532-3540, 2013.

Ding D., Chong X., Xiao G., Lv L., Lei C., Luo J., Zang, Y., Combustion synthesis of $B_4C/Al_2O_3/C$ composite powders and their effects on properties of low carbon MgO-C refractories. Ceramics International 45(13), 16433-16441, 2019.

Domnich V., Reynaud S., Haber R. A., Chhowalla M., Boron carbide: structure, properties, and stability under stress. Journal of the American Ceramic Society 94(11), 3605-3628, 2011.

He P., Dong S., Kan Y., Zhang X., Ding Y., Microstructure and mechanical properties of B_4C–TiB_2 composites prepared by reaction hot pressing using Ti_3SiC_2 as additive. Ceramics International 42(1), 650-656, 2016

He Q., Xie J., Wang A., Liu C., Tian T., Hu L., Fu Z., Effects of boron content on the microstructures and mechanical properties of reactive hot-pressed B_xC-TiB_2-SiC composites. Ceramics International 45(16), 19650-19657, 2019.

Liu Y., Wu X., Liu M., Huang Y., Huang Z., Microstructure and mechanical properties of B_4C–TiB_2–SiC composites fabricated by spark plasma sintering. Ceramics International 46(3), 3793-3800, 2020.

Munir Z. A., Anselmi-Tamburini U., Ohyanagi M., The effect of electric field and pressure on the synthesis and consolidation of materials: a review of the spark plasma sintering method. Journal of Materials Science 41(3), 763-777, 2006.

Skorokhod V., Vlajic M. D., Krstic V. D., Mechanical properties of pressureless sintered boron carbide containing TiB 2 phase. Journal of materials science letters 15(15),1337-1339,1996.

Song Q., Zhang Z. H., Hu Z. Y., Yin S. P., Wang H., Li X. Y., Cheng X. W., Influences of the pre-oxidation time on the microstructure and flexural strength of monolithic B_4C ceramic and TiB_2-SiC/B_4C composite ceramic. Journal of Alloys and Compounds 831, 154852, 2020.

Thevenot F., Boron carbide—a comprehensive review. Journal of the European Ceramic Society 6(4), 205-225, 1990.

Wen Q., Tan Y., Zhong Z., Zhang H., Zhou X., High toughness and electrical discharge machinable B4C-TiB2-SiC composites fabricated at low sintering temperature. Materials Science and Engineering: A 701, 338-343, 2017.

Ye F., Hou Z., Zhang H., Liu L., Densification and mechanical properties of spark plasma sintered B_4C with Si as a sintering aid. Journal of the American Ceramic Society 93(10), 2956-2959, 2010.

Yin S. P., Zhang Z. H., Cheng X. W., Su T. J., Hu Z. Y., Song Q., Wang H., Spark plasma sintering of B_4C-TiB_2-SiC composite ceramics using B_4C, Ti_3SiC_2 and Si as starting materials. Ceramics International 44(17), 21626-21632, 2018.

Zhang X., Zhang Z., Wang W., Shan J., Che H., Mu J., Wang G., Microstructure and mechanical properties of B_4C–TiB_2–SiC composites toughened by composite structural toughening phases. Journal of the American Ceramic Society 100(7), 3099-3107, 2017.